Heliyon 6 (2020) e04647

Contents lists available at ScienceDirect

Heliyon

journal homepage: www.cell.com/heliyon

Review article

Study of the structural, chemical descriptors and optoelectronic properties of the drugs Hydroxychloroquine and Azithromycin

G.W. Ejuh [a,b,*], C. Fonkem [c], Y. Tadjouteu Assatse [c], R.A. Yossa Kamsi [c], Tchangnwa Nya [d], L.P. Ndukum [e], J.M.B. Ndjaka [c]

[a] University of Bamenda, National Higher Polytechnic Institute, Department of Electrical and Electronic Engineering, P. O. Box 39 Bambili, Cameroon
[b] University of Dschang, IUT-FV Bandjoun, Department of General and Scientific Studies, P.O. Box 134, Bandjoun, Cameroon
[c] University of Yaoundé I, Faculty of Science, Department of Physics, P.O. Box 812 Yaounde, Cameroon
[d] University of Maroua, Faculty of Science, Department of Physics, P.O. Box 814 Maroua, Cameroon
[e] University of Bamenda, National Higher Polytechnic Institute, Department of Computer Engineering, P. O. Box 39 Bambili, Cameroon

ARTICLE INFO

Keywords:
Pharmaceutical chemistry
Azithromycin
Hydroxychloroquine
COVID-19
Chemical descriptors
Optoelectronic devices
Nonlinear optical application

ABSTRACT

Density functional theory (DFT) was performed in order to predict the structural, chemical descriptors and optoelectronic properties of the drugs Hydroxychloroquine and Azithromycin using the wB97XD, O3LYP and B3LYP functional with 6-31+G(d,p) basis set. It is observed from our studies that most of the descriptors presented show association with some processes, including absorption, blood-brain barrier transport, binding and even toxicity. Hence, the treatment of COVID-19 using Hydroxychloroquine and Azithromycin in some patients as single dose and their combination in patients with Corona virus resistance can be more effective. Our results show that these therapeutic molecules may also have good nonlinear optical applications, may have semiconductor character with wide band gap and can also be promising materials in the production of optoelectronic devices. The density of states and thermodynamic properties were equally determined.

1. Introduction

COVID-19 is an emerging disease due to a novel coronavirus named as SARS-CoV-2, which started in Wuhan, China in 2019 and spread to the other continents [1, 2]. It was declared to be pandemic in 2020 by the World health Organization [3]. Haman Corona viruses which belong to the family of Coronaviridae were first identified and observed in 1960 [4, 5]. Corona viruses are enveloped-single stranded-positive sense RNA virus. COVID-19 is a new form of corona virus which is round in shape with a diameter of approximately 60–120 nm [6] and with an incubation period [5]. Among potential drugs to treat COVID-19, repositioning of old drugs such as Chloroquine, Hydroxychloroquine, Azithromycin, Remdesivir etc for use as antiviral treatment is an interesting strategy because knowledge on their mode of action, safety profile, side effects, dosage and their interactions with other biological molecules are well known [7, 8, 9]. This study is limited to Hydroxychloroquine and Azithromycin.

Hydroxychloroquine is a drug derived from 4-aminoquinoline. It is used as an antimalarial drug ever since the Second World War. It is also widely used in the treatment of lupus erythematosus, rheumatoid arthritis, and other inflammatory and skin diseases [10, 11, 12, 13, 14]. Hydroxychloroquine is rapidly absorbed by the intestine, accumulating in organs such as the liver, spleen, lungs and kidneys. It is partially converted to active metabolites in the liver and excreted primarily through the kidney when ingested [15]. According to literature [12, 16, 17, 18], some risk factors increase the likelihood of retinopathy caused by Hydroxychloroquine; for instance, the daily dosage, the cumulative dose, and renal or liver disease, besides age and previous retinal diseases. Thus, pharmaceuticals containing Hydroxychloroquine must undergo strict quality control, which requires the development of simple, rapid, and accurate analytical procedures for the identification and quantification of this drug in both pharmaceutical and biological samples. Gautret et al. 2020 [19] conducted a clinical trial aiming at assessing the effect of hydroxychloroquine on SARS-CoV-2-infected patients after approval by the French Ministry of Health. In their report, they focused on the virological data in patients receiving hydroxychloroquine as compared to a control group. Their results showed that, Hydroxychloroquine is efficient in eliminating viral nasopharyngeal carriage of SARS-CoV-2 in COVID-19 patients in only three to six days, in most patients and a significant difference was observed between

* Corresponding author.
E-mail address: gehwilsonejuh@yahoo.fr (G.W. Ejuh).

https://doi.org/10.1016/j.heliyon.2020.e04647
Received 28 May 2020; Received in revised form 29 June 2020; Accepted 3 August 2020

Hydroxychloroquine-treated patients and controls starting even on day 3 post-inclusion. Their results also suggested a synergistic effect of the combination of hydroxychloroquine and Azithromycin. They recommended that patients with COVID-19 should be treated with Hydroxychloroquine and Azithromycin to cure their infection and to limit the transmission of the virus to other people in order to curb the spread of COVID-19 in the World. Equally, they proposed that further studies should be carried out on this combination because such combination can both act as an antiviral therapy against SARS-CoV-2 and prevent bacterial super-infections. Hydroxychloroquine which is an analogue of Chloroquine has demonstrated to have an anti-SARS-CoV activity in vitro [20]. Even though Chloroquine has proven to have an inhibitor effect on the growth of SARA-CoV-2 in vitro, the clinical safety profile of Hydroxychloroquine is better than that of Chloroquine (during long-term use) and allows higher daily dose [21] and has fewer concerns about drug-drug interactions [22].

Azithromycin is a macrolide antibiotic which differs chemically from erythromycin by methyl-substituted nitrogen atom in the macrolide ring. It is composed of fifteen-membered ring structure having two sugar moieties, several hydroxyl groups, two tertiary amino groups, and one oxycarbonyl group [23]. Azithromycin launched in 1991 has become one of the most widely used antimicrobials [24]. Favorable pharmacological properties such as acid resistance, a short time to achieve peak concentrations with an up to 800-fold accumulation in phagocytes at the infection site, and long half-life allowing a large single oral dose to maintain bacteriostatic activity in the infected tissue for 4 days have contributed to the success of Azithromycin as an antibiotic [25, 26, 27]. Clinical studies have demonstrated that patients suffering from both intermittent and chronic pseudomonas aeruginosa infection, e.g., cystic fibrosis (CF), chronic obstructive pulmonary disease (COPD), and diffuse panbronchiolitis (DPB), were treated using Azithromycin [28, 29]. Studies by some researchers, have shown that Azithromycin concentrations are highly accumulated in alveolar macrophages and lung which is 100% higher than that reported in plasma [23, 30]. Based on these studies, Azithromycin has been largely recommended for the treatment of some respiratory diseases, sexually transmitted diseases, some skin diseases, and otitis media [23, 31]. Among other reasons, this antibiotic formulated mainly as suspension or tablets is used in human and in veterinary medicine [23]. Kumar and Park, 2011 [32] reported Azithromycin to be a new chiral selector in capillary electrophoresis studies with multiple stereogenic centers. Due to the presence of different functional groups and multiple chiral centers, Azithromycin may undergo multiple interactions with the analyte enantiomeric molecules [32], biological molecules and with the enzymes produce by COVID-19 for chiral recognition. Recently, the drugs stereochemistry has become a significant issue in the pharmaceutical industry. The stereoisomers interact differently with the macromolecules in the body, while waiting for the process of passive diffusion and transporters uptake into cell membranes which is equivalent for both moieties [33, 34, 35]. Imperi et al. 2014 [36] studied the antivirulence activity of Azithromycin in Pseudomona aeruginosa. In their studies, they showed that besides the growth-inhibiting activity of Azithromycin, Azithromycin has potent anti-inflammatory properties, as well as antivirulence activity on some intrinsically resistant bacteria, such as pseudomonas aeruginosa. The antivirulence activity of this molecule mainly relies on its ability to interact with the ribosome, resulting in direct and/or indirect repression of specific subsets of genes involved in virulence, quorum sensing, biofilm formation, and intrinsic antibiotic resistance in the bacterium.

Most drugs and drug-like molecules are likely to bind to multiple transporters, for example; drugs are known to interact with no fewer than six targets and many proteins are known to interact with hundreds of drugs to get the biophase [37]. Hence, the differences in active transport in serum secretion protein-binding, metabolism, and pharmacological effects for both Hydroxychloroquine and Azithromycin may have differences for achieving the biophase. Therefore, a combination of Hydroxychloroquine and Azithromycin for the treatment of COVID-19 is significantly more efficient for the elimination of the corona Virus as reported in literature [19]. Azithromycin has shown to be active in vitro against Zika and Ebola viruses [38, 39, 40] and to prevent severe respiratory tract infections when administrated to patients suffering from viral infection [41]. Hence, we can say that the molecules Hydxoxychloroquine and Azithromycin have many important biological characteristics including antibacterial, antifungal, immunomodulatory properties and antivirulence activity.

From structural studies [42, 43, 44] and experimental studies [44, 45, 46], SARS-CoV-2 appears to bind to the human receptor acethyl choline esterase 2 (ACE2) and the spike protein of SARS-CoV-2 has a functional polybasic (furin) cleavage site. Based on these studies, SARS-CoV-2 seem to have a receptor-binding domain that binds with high affinity to ACE2 from humans, ferrets, cats and other species with high receptor homology [42]. The SARS-CoV-2 main protease structure (Mpro) was first released to the Protein Data Bank, on March 2020 [47]. Proteases are central enzymes in the biology of humans and viruses, and several of them have become drug targets for anti-viral therapy as well as for the treatment of various diseases. There is a number of approved drugs that act as protease inhibitors [20]. SARS-CoV-2 main protease is a cysteine protease [48, 49] and it cleaves the viral polyprotein at no less than 11 sites [47]. It implies SARS-CoV-2 can easily bind with other molecules with high binding affinity. In this regard, we want to study the physico-chemical properties of the molecules Hydroxychloroquine and Azithromycin which are used for treatment of the COVID-19 which is ravaging the World. Furthermore, we want to determine the chemical descriptors of these molecules so as to see if they correlate with experimental and other theoretical results given in literature. We also want to determine the optoelectronic properties and spectra of these molecules. Some of the important electronic properties such as electrophilicity index, global hardness, chemical potential, ionization potential, electron affinity, dipole moment, polarizability, anisotropy and hyperpolarizability will be determine so as identify the nature of the pharmacological properties of these molecules [50, 51]. Most of these properties are use in quantitative structural analysis relationship (QSAR) and drug design [52, 53, 54].

2. Computational methods

The optimized molecular structures, structural properties, thermochemical properties, vibrational frequencies and electronic properties of Hydroxychloroquine and Azithromycin were calculated using the Gaussian 09 quantum chemical program [55] and the Gauss view visualization program [56]. Firstly, the optimized molecular structures of the molecules were performed using by 6-31+G(d,p) basis set with the WB97XD, O3LYP and B3LYP functional. Secondly, the vibrational frequencies were determined and their fundamental vibrational modes were characterized by their potential energy distribution. Finally, based on the optimized structures, some of physical and chemical properties were calculated.

Quantum mechanical methods have proven to be very accurate in generating molecular geometries and in the prediction of relative conformational energies, and have become a useful tool in drug related computational research [57]. It has also found application in prediction of transition state properties, reactivity and enzyme mechanism studies, and in the investigations of drug-receptor and protein-ligand interactions and binding energies [57]. Furthermore, the use of these methods permit us to determine accurately a wide range of molecular descriptors including dipole moment, ionization potential and electron affinity, which are accessible only through quantum mechanical calculations [58, 59, 60, 61]. As a result, the molecular properties determined by DFT and

other quantum mechanical method are often used in quantitative structure-activity and structure-property relationship models.

3. Results and discussion

3.1. Optimized molecular structure and geometric parameters of the molecules

3.1.1. Optimized molecular structures of Hydroxychloroquine and Azithromycin

The optimized molecular structures of the molecules Hydroxychloroquine and Azithromycin are reported in Figure 1.

3.1.2. Optimized geometrical parameters of Hydroxychloroquine and Azithromycin

The geometrical parameters of the molecules that is the bond lengths and bond angles of Hydroxychloroquine and Azithromycin are given in Table S1 and Table S2 respectively of the supplementary materials. We observe a slight difference between the geometric parameters calculated with the B3LYP, O3LYP and wB97XD functional. The wB97XD functional differs significantly from the B3LYP and the O3LYP functional by the long range interaction which is taken into account in the geometric optimization. Thus, the addition of dispersion effects does not significantly influence the structural parameters of these molecules. In order to validate the optimized geometrical structure of Hydroxychloroquine, a comparison of some calculated properties is carried out with the experimental results of Hydroxychloroquine sulfate [62]. It should be noted that the geometric orientation of the groups of atoms of Hydroxychloroquine present in this research work is similar to that of Hydroxychloroquine found in Hydroxychloroquine sulfate. The calculated C–C, C–N, C–O and C–Cl bond lengths are in good agreement with the experimental values reported in literature. Similarly, the calculated bond angles are in good agreement with the experimental values reported in literature [62]. These results show that the optimized geometrical structure of Hydroxychloroquine is valid.

Frequency analysis was performed to verify the stability of the optimized structures. Figure 2 shows the IR and Raman spectra of hydroxychloroquine and those of Azithromycin are shown in Figure 3. As shown in these spectra, no imaginary frequencies were observed. This means that local minima was reached at the end of the optimization.

3.2. Quantum chemical descriptors of the molecules

The molecular descriptors of interest in our research are LUMO-HOMO energy band gap (E_g), ionization potential, electron affinity (EA), chemical potential (ϑ), chemical hardness (κ), chemical softness (S), electronegativity (δ), electrophilicity index (ω), dipole moment (μ_{tot}), average polarizability (α_0), related anisotropy ($\Delta\alpha$) and first order hyperpolarizability (β_0) of the molecules which have been predicted using the wB97XD, O3LYP and B3LYP functional and are given in Table 1. Whereas the dipole moment and polarizability represent information about charge distribution within the molecule, and therefore affect solvation and the molecule's membrane permeability, the ionization potential and electron affinity supply information regarding molecule's stability, which could also find a reflection in drug's metabolism [63]. Based on studies found in literature, which shows that increase in polarity, polarizability and the ability for hydrogen bonding strongly reduced brain penetration [64] which is in accord with our results. The polarity of the molecules, represented mostly by a dipole moment is the most important factor in inhibition activity, where the activity increases with increasing dipole moment. Equally, studies have shown that binding to an active pocket of some receptor depends on the electronic structure of the ligand, with a significant contribution from dipole moment and polarizability [65]. This may be due an electrostatic field generated by the receptor, and therefore would affect more strongly and interact with molecules which have a higher dipole moment or polarizability [66]. Moreover, drugs with greater dipole moment are less well absorbed while those with high electron affinity are most important for intestinal absorption [67]. From Table 1, it is observed that the dipole moments values of these molecules are within the range $3D < \mu < 5D$ which corroborate with μ values of most drugs given in literature [68]. From these μ values of the molecules, it implies the molecules have high absorption and are actively transported.

We equally observed from Table 1 that the polarizability values of the molecules are less than 5 A^{o3}

(1 $au^3 = (0.529)^3$ $Å^3$) [69] which implies Hydroxychloroquine and Azithromycin have good membrane permeability as documented in literature [68]. Though polarizability, hyperpolarizability and hyper-order electric moments can be used to study the toxicity of drugs, polarizability is the main factor influencing the binding affinity of the drug. This can be explained by the fact that polarizability is a representation of molecular hydrophobicity [70]. Hence, the large values of the

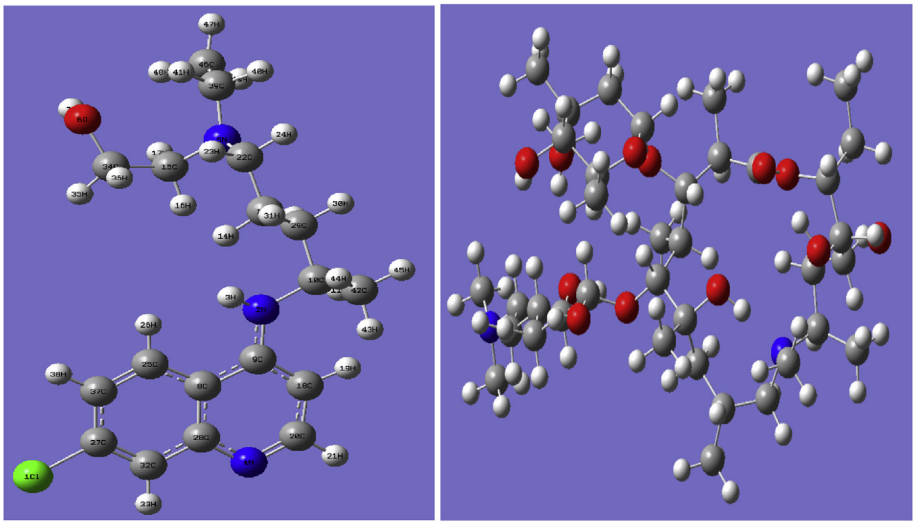

Figure 1. Optimized geometric structures of Hydroxychloroquine (A) and Azithromycin (B).

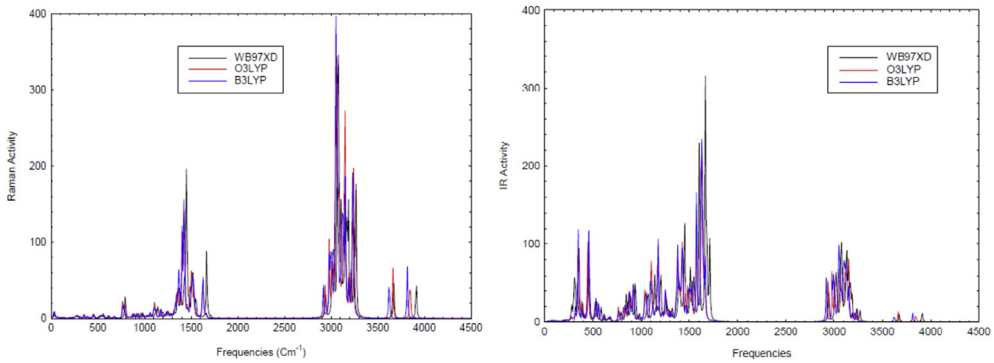

Figure 2. wB97XD, O3LYP and B3LYP infrared (IR) (Right) and Raman spectra of Hydroxychloroquine (Left). The spectra lines in black represent the spectra obtained at the wB97XD, that in red for O3LYP and that in blue for the B3LYP.

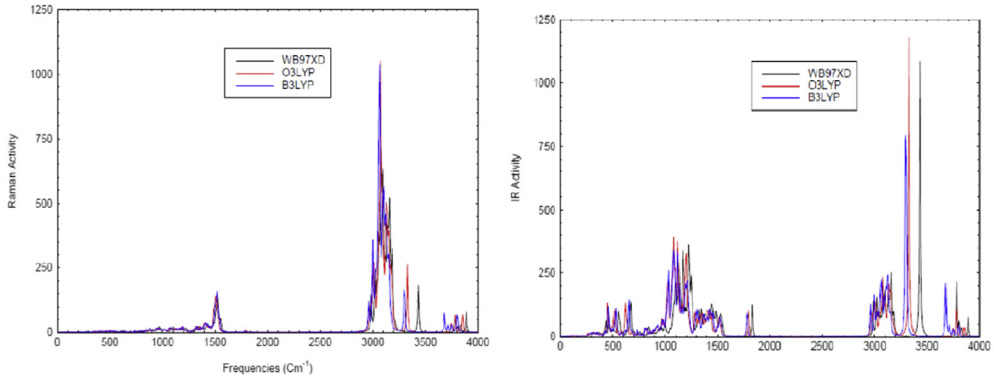

Figure 3. wB97XD, O3LYP and B3LYP infrared (IR) (Right) and Raman spectra of Azithromycin (Left). The spectra lines in black represent the spectra obtained at the wB97XD, that in red for O3LYP and that in blue for the B3LYP.

polarizability of the molecules show that the molecules have high binding affinity.

The frontier molecular orbitals which can give realistic qualitative information about susceptibility of the electrons of the HOMO to transfer to the LUMO were also determined. Moreover, HOMO and LUMO are very important quantum chemical parameters to determine the reactivity of the molecules and are used to calculate many important parameters such as the chemical reactivity descriptors. These orbitals control the mode of the interaction of the drugs with other molecules such as the interactions between these drugs and their receptors. The ionization potential and electron affinity were determined by using HOMO and LUMO energies. The HOMO and LUMO plots of Hydroxychloroquine and Azithromycin are shown in Figures 4 and 5 while the plots of their density of states (DOS) are presented in Figures 6 and 7 respectively. The data of molecular orbitals use to plot the density of states (DOS) have been obtained with the help of GaussSum 2.2 Program [71]. The density

Table 1. HOMO and LUMO molecular orbital energies, LUMO-HOMO Energy band gap (E_g), Ionization potential, electron affinity (EA), chemical potential (ϑ), chemical hardness (κ), chemical softness (S), electronegativity (δ), electrophilicity index (ω), dipole moment (μ_{tot}), average polarizability (α_0), related anisotropy ($\Delta\alpha$) and first order hyperpolarizability (β_0) of the molecules.

Molecule	Hydroxychloroquine			Azithromycin		
Parameters	B3LYP	WB97XD	O3LYP	B3LYP	WB97XD	O3LYP
E_{HOMO} (eV)	-5.517	-7.652	-4.930	-5.327	-7.471	-4.726
E_{LUMO} (eV)	-1.220	0.549	-1.376	-0.127	1.953	-0.220
E_g (eV)	4.297	8.201	3.554	5.200	9.424	4.506
IP (eV)	5.517	7.652	4.930	5.327	7.471	4.726
EA (eV)	1.220	-0.549	1.376	0.127	-1.953	0.220
ϑ	-3.369	-3.552	-3.053	-2.727	-2.759	-2.473
κ	2.149	4.101	1.777	2.600	4.712	2.253
S	0.465	0.243	0.563	0.385	0.212	0.444
δ	3.369	3.552	3.053	2.727	2.759	2.473
ω	2.641	1.538	2.797	1.430	0.808	1.357
α_0 x 10^{-41} $C^2m^2J^{-1}$	384.296	374.919	386.045	752.925	734.554	754.412
$\Delta\alpha$ x10^{-41} $C^2m^2J^{-1}$	958.737	933.751	963.754	168.207	161.274	167.544
μ_{tot} x10^{-29} Cm	1.731 (5.188D)	1.762 (5.284D)	1.804 (5.410 D)	1.104 (3.3097D)	1.166 (3.4945D)	1.099 (3.2949D)
M_R x10^{-14} x 10^{-14} $C^2m^2J^{-1}mol^{-1}$	9.686	9.449	9.730	1.898	1.851	1.901
β_0 x 10^{-52} $C^3m^2J^{-2}$	116.346	107.100	123.568	50.162	43.881	66.247

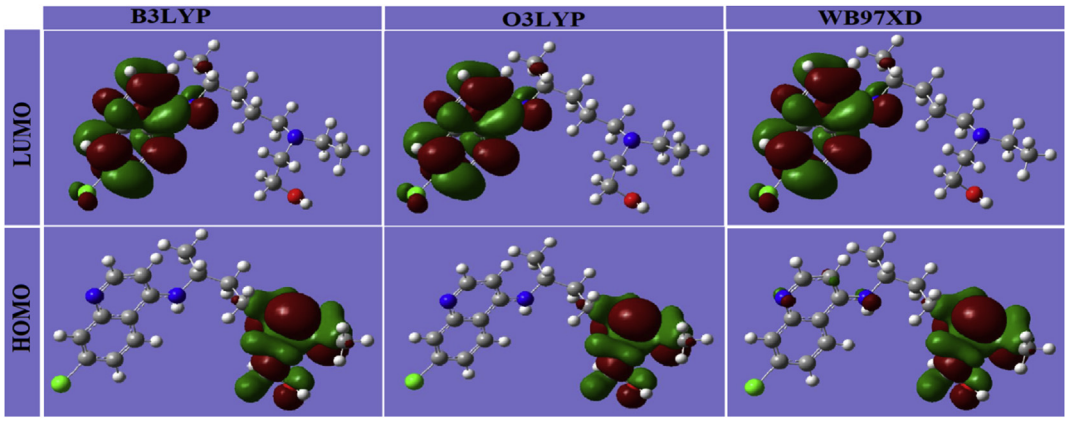

Figure 4. HOMO – LUMO Molecular orbitals of Hydroxychloroquine obtained using the B3LYP, O3LYP and WB97XD functional with the 6-31+G(d,p).

of state presented in Figures 6 and 7 are restricted to some occupied and unoccupied molecular orbitals around the HOMO and LUMO molecular orbitals. Interestingly, the large energy gap of the molecules tell us that there are many hydrophilic interactions that could facilitate the binding with the receptors. This suggests that such hydrophilic interactions considerably impact the binding affinity of these drugs to the receptors. During the binding process, the HOMO of a certain drug and the LUMO with the adjacent residues could share the orbital interactions [5]. The large HOMO-LUMO energy gaps obtained in our studies also reveal to us that the molecules have high excitation energies and good stability [72]. The electron affinity which is used for the investigation of optimal bioavailability [73] and ionization potential which is related to the blood-brain barrier permeation [74] are also reported in Table 1. The values of the IP and EA of the molecules are within the range of values given in literature for most drugs 1.5 eV $<$ EA $<$ 2 eV for EA and 6 eV $<$ IP $<$ 9 eV for the IP [68]. Molecules with high IP are equally characterized by high EA, showing that IP filter might not have any additional influence once the EA filter is applied.

The values of the dipole moment, polarizability, ionization potential and electron affinity are approximately equal those reported in literature [68]. Hence, it is observed from our studies that most of the descriptors of interest presented above show association with some processes, including absorption, blood-brain barrier transport, binding and even toxicity.

3.3. Nonlinear properties of Hydroxychloroquine and Azithromycin

The Nonlinear optical properties such as dipole moment, average polarizability, related anisotropy, molar refractivity and first order hyperpolarizability of the molecules are also among the quantum chemical descriptors of the molecules. Nonlinear properties are very important in pharmacology. Indeed, the two main characteristics that govern interactions between drugs and biological molecules are spatial structure and electronic distribution. The polarity of a molecule comes from the non-homogeneous distribution of its electronic cloud. Polarizability refers to the ease with which the electronic cloud of a molecule can be moved under the effect of an electric field or another molecule. Therapeutic molecules can also be exploited for applications in nonlinear optics. The incorporation of an organic molecule into nonlinear optical materials is usually performed by comparing its dipole moment, average polarizability, hyperpolarizability value with that of a prototype molecule such as urea and 3-methyl 4-nitropyridine 1-oxide. The nonlinear properties such as dipole moment, average polarizability, first order hyperpolarizability and molar refractivity of hydroxychloroquine and Azithromycin are reported in Table 1. The large values of the dipole moment, average polarizability, first order hyperpolarizability and the molar refractivity of Hydroxychloroquine and Azithromycin are much higher than that of urea [75, 76] and therefore these therapeutic molecule may also have good nonlinear optical applications.

Electronic properties such as HOMO energy, LUMO energy and the HOMO-LUMO energy gap are also given in Table 1. The energy gap is a very important index of stability with respect to external electromagnetic radiation. It also provides information on the conductive, semiconducting or insulating nature of a material. As shown in Figures 6 and 7 the energy gap of Hydroxychloroquine and Azithromycin decreases slightly when we move from B3LYP to O3LYP level. However, when dispersion effects are introduced into electronic property calculations, a very large increase in the energy gap value is observed. The value obtained with the wB97XD is almost double the value obtained with the B3LYP which may be due to the dispersion effect at the level of the

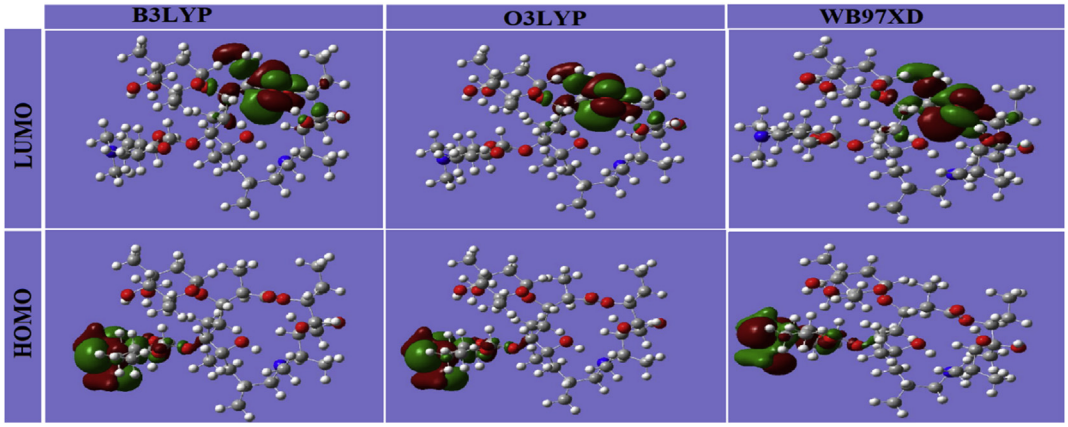

Figure 5. HOMO – LUMO Molecular orbitals of Azithromycin obtained using the B3LYP, O3LYP and WB97XD functional with the 6-31+G(d,p).

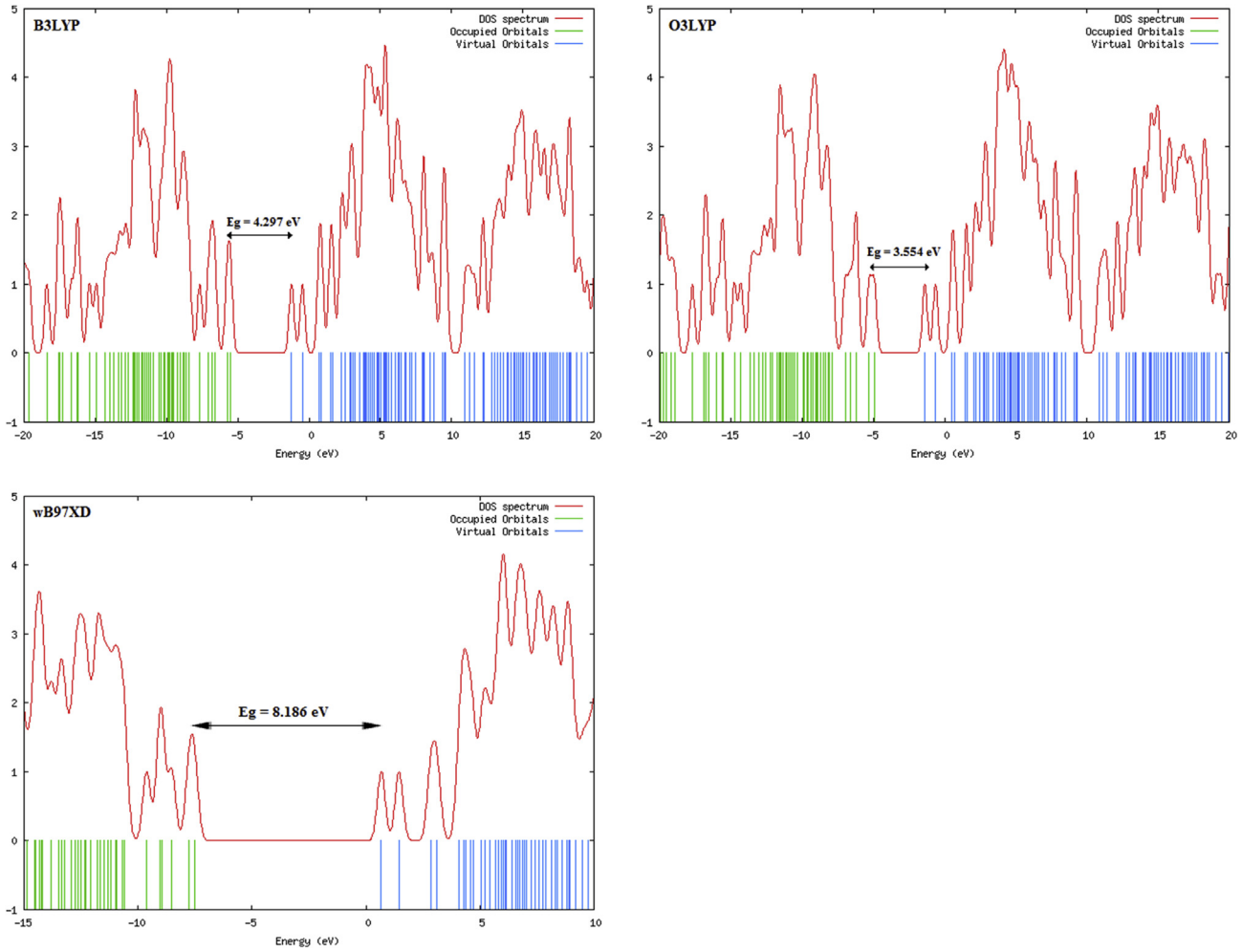

Figure 6. Density of states (DOS) of Hydroxychloroquine obtained obtained using the B3LYP, O3LYP and WB97XD functional with the 6-31+G(d,p) respectively.

wB97XD functional. Several research works reported in the literature [75, 76, 77, 78, 79] have shown that the B3LYP functional gives good energy gap results. Thus, by increasing the accuracy of calculation, the energy gap would be lower as can be observed with the value obtained with the B3LYP functional compared to that obtained with the wB97XD functional. Even though the energy gap values are high for these molecules, it permit us to say that the molecules Hydroxychloroquine and Azithromycin may have semiconductor character with wide band gap and therefore a high stability index.

3.4. Optoelectronic properties

The optoelectronic properties such as dielectric constant, electrical susceptibility and refractive index of the molecules are grouped in Table 2. These properties were determined using formulae reported in the literature [75, 76, 77, 78, 79]. The values of the dielectric constant, the electric susceptibility and the refractive index computed with B3LYP functional are lower than the values obtained with the O3LYP and wB97XD functional for Hydroxychloroquine and vice versa for Azithromycin. The small value of the dielectric constant and the large values of the electric susceptibility and refractive index of hydroxychloroquine indicate that the molecules Hydroxychloroquine and Azithromycin can also be promising materials in the production of optoelectronic devices [80].

3.5. Thermochemical properties of Hydroxychloroquine and Azithromycin

The enthalpy, Gibbs free energy, entropy and heat capacity at constant pressure of Hydroxychloroquine molecule are presented in Table 3. The results presented in this table correspond to standard temperature and pressure conditions. The values obtained with B3LYP vary when we move to O3LYP or wB97XD functional. Temperature is a very important thermodynamic parameter in the production, storage and use of therapeutic molecules. For this reason, the effect of temperature on the calculated thermodynamic properties was examined. Figure 8 shows the variation curves of standard thermodynamic properties H, G, S and C_p with temperature of the Hydroxychloroquine molecule while Figure 9 gives that of Azithromycin. The temperature range is limited from 175 K to 330 K so that the lower bound is close to the minimum temperature of the globe, while the upper bound is close to the maximum temperature of the globe. As shown in Figures 8 and 9, the values of H, S and Cp increase, while the values of G decrease with increasing temperature. A key part of drug design and development is the optimization of molecular interactions between an engineered drug candidate and its binding target. Thermodynamic characterization provides information about the balance of energetic forces driving binding interactions and is essential for understanding and optimizing molecular interactions [81]. The crucial parameter describing the interaction of binding partners is the free energy where both the magnitude and sign describe the likelihood of

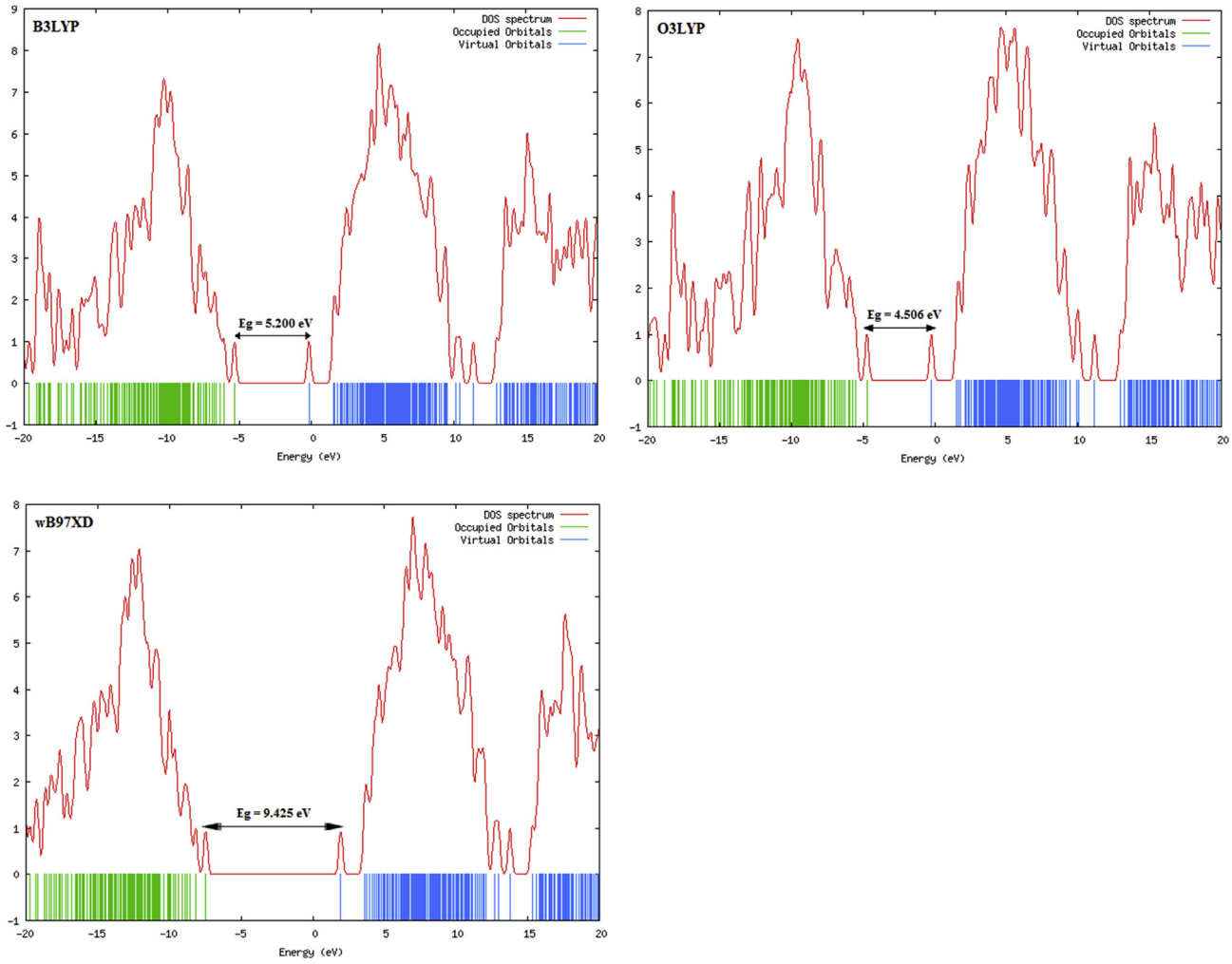

Figure 7. Density of states (DOS) of Azithromycin obtained obtained using the B3LYP, O3LYP and WB97XD functional with the 6-31+G(d,p) respectively.

Table 2. Volume V (m^3), average field E (V m^{-1}), polarization density P (Cm^{-2}), electric susceptibility χ, dielectric constant ε_r, displacement vector D ($C^2m^2J^{-2}$) and refractive index η.

Hydroxychloroquine							
Méthode	$Vx10^{-28}m^3$	$E_{ch}x10^{10}$	P	χ	ε_r	η	D
B3LYP	1.785	4.504	0.097	2.432	3.432	1.853	0.137
WB97XD	1.673	4.700	0.105	2.523	3.523	1.877	0.147
O3LYP	1.664	4.673	0.108	2.610	3.610	1.900	0.149
Azithromycin							
B3LYP	3.400	0.147	0.032	2.459	3.459	1.860	0.045
WB97XD	3.971	0.159	0.029	2.060	3.060	1.749	0.043
O3LYP	3.701	0.146	0.030	2.321	3.321	1.822	0.043

Table 3. Standard enthalpy H (KJ/mol), standard Gibbs free energy G (KJ/mol), standard entropy S (J/mol.K) and heat capacity at constant pressure Cp (J/mol.K) of Hydroxychloroquine and Azithromycin.

Hydroxychloroquine					Azithromycin			
Method	H $x10^3$ kJ/mol	G $x10^3$ kJ/mol	S J/mol.K	C_p J/mol.K	H $x10^3$ kJ/mol	G $x10^3$ kJ/mol	S J/mol.K	C_p J/mol.K
B3LYP	-3677.891	-3678.104	708.866	384.110	-6570.301	-6570.690	1303.250	958.630
wB97XD	-3677.087	-3677.297	702.402	378.401	-6568.608	-6568.980	1247.361	936.791
O3LYP	-3676.924	-3677.138	717.719	386.150	-6567.705	-6568.098	1317.251	963.630

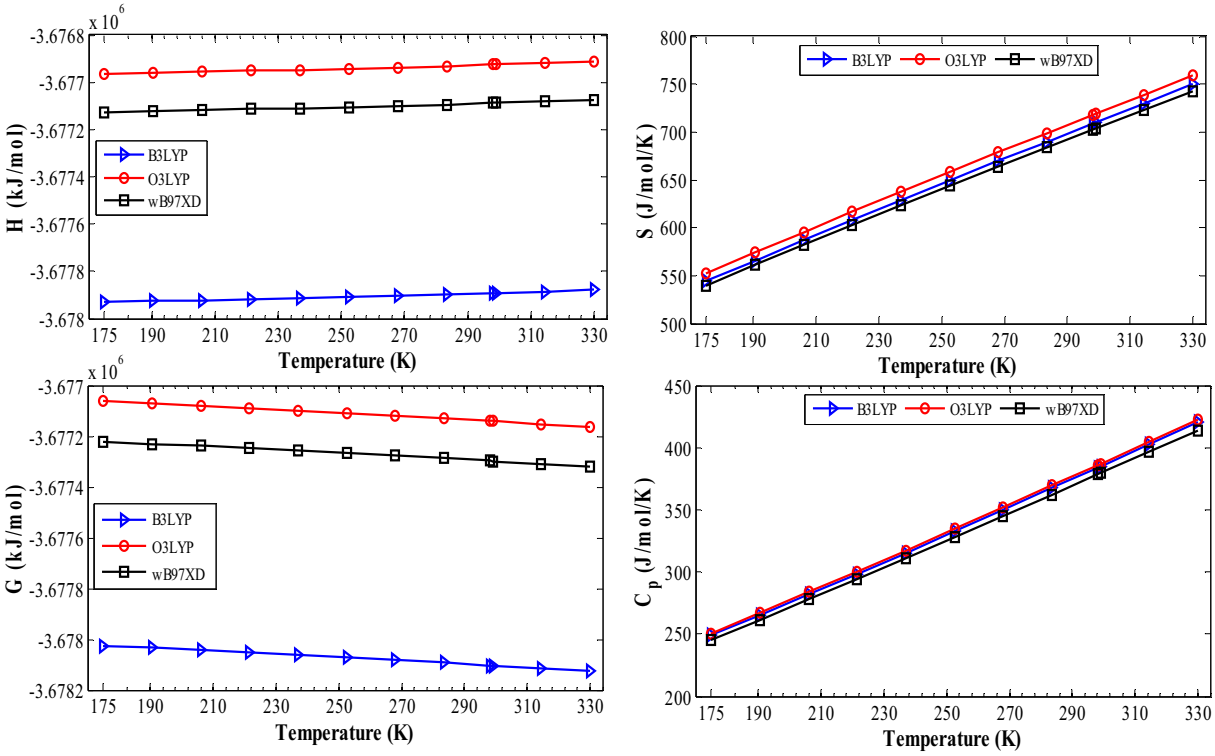

Figure 8. Plots of H (Left upper), G (Left lower), S (Right upper) and Cp (Right lower) with temperature of Hydroxychloroquine.

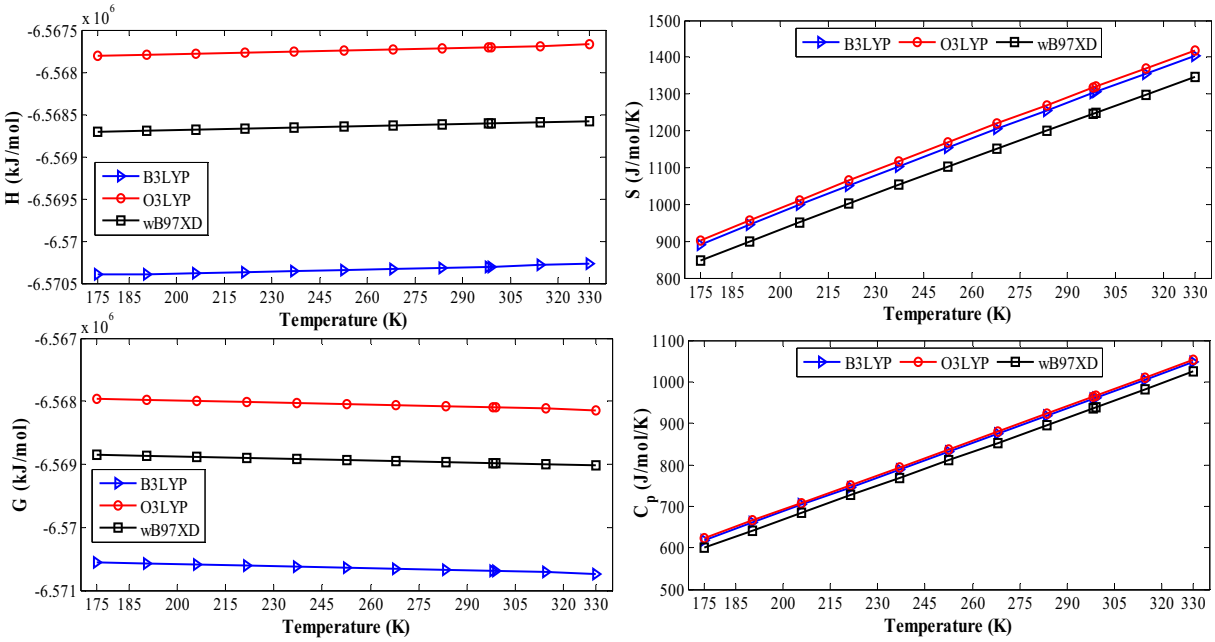

Figure 9. Plots of H (Left upper), G (Left lower), S (Right upper) and Cp (Right lower) with temperature of Azithromycin.

biomolecular events occurring. The large negative values of G signifies that the molecules have higher affinity. The free energy is made of the enthalpy and the entropy. Enthalpy reflects heat differences between reactants and products of a binding reaction as a result of net bond formation or breakage, with negative values indicating a net release of heat energy with the resulting products at a lower energy level than the reactants [81] and variation of enthalpy with temperature at constant temperature gives the C_p. Entropy reveals the ease of distribution of binding energy among molecular energy levels with positive values associated with an increase in disorder, and vice versa.

A negative *Cp* indicates that the binding complex has a lower heat capacity than the free binding partners and, along with a positive entropy. This is typically associated with hydrophobic interactions and conformational changes upon binding [82, 83]. Hence, these results are very important thermochemical information in pharmacology.

4. Conclusion

Based on structural and experiments studies, SARS-CoV-2 appears to bind to the human receptor acethyl choline esterase 2 (ACE2) and the spike protein of SARS CoV-2 has a functional polybasic (furin) cleavage site. From these studies, SARS-CoV-2 seem to have a receptor-binding domain that binds with high affinity to ACE2 from humans, ferrets, cats and other species with high receptor homology. Thus, due the high-affinity binding of the SARS-CoV-2 spike protein to human ACE2 and from the high binding affinity of both Hydroxychloroquine and Azithromycin implies that these molecules can easily bind together. Hence, the treatment of COVID-19 using Hydroxychloroquine and Azithromycin in some patients as single dose and their combination in patients with Corona virus resistance can be more effective. It is also observed from our studies that most of the descriptors of interest presented above show association with some processes, including absorption, blood-brain barrier transport, binding and even toxicity. From the parameters determined, we can conclude that these parameters together all affect the degree of the binding affinity of Hydroxychloroquine and Azithromycin with the active protein sites to afford a certain degree of inhibition thereby preventing the entrance and formation of the viral particles. The calculations were carried out by relaxing the structures of the molecules.

Equally, the key thermodynamic parameters of the molecules are the binding free energy (G), enthalpy (H), entropy (S) and heat capacity change (Cp). G indicates the likelihood and extent of biomolecular interactions and is composed of H and S components, which define the molecular forces governing the binding process. It is the balance of these forces that determines the overall thermodynamics of molecular interactions.

Furthermore, from the large values of the dipole moment, average polarizability, first order hyperpolarizability and the molar refractivity of Hydroxychloroquine and Azithromycin, we are tempted to say that these therapeutic molecule may also have good nonlinear optical applications and may equally have semiconductor character with wide band gap due to the large energy gap.

Furthermore, from the small value of the dielectric constant, the large values of the electric susceptibility and refractive index of Hydroxychloroquine and Azithromycin indicate that these molecules can also be promising materials in the production of optoelectronic devices.

Declarations

Author contribution statement

All authors listed have significantly contributed to the development and the writing of this article.

Funding statement

This research did not receive any specific grant from funding agencies in the public, commercial, or not-for-profit sectors.

Competing interest statement

The authors declare no conflict of interest.

Additional information

Supplementary content related to this article has been published online at https://doi.org/10.1016/j.heliyon.2020.e04647.

Acknowledgements

We are thankful to the Council of Scientific and Industrial Research (CSIR), India for financial support through Emeritus Professor scheme (grant no. 21(0582)/03/EMR-II) to Late Prof. A.N. Singh of the Physics Department, Bahamas Hindu University, India which enabled him to purchase the Gaussian Software. We are most grateful to late Emeritus Prof. A.N. Singh for donating this software to Prof Geh Wilson Ejuh, and to the Materials Science Laboratory of the University of Yaoundé I for enabling us used their computing facilities.

References

[1] C.C. Lai, T.P. Shih, W.C. Ko, H.J. Tang, P.R. Hsueh, Severe acute respiratory syndrome coronavirus 2 (SARS-CoV-2) and coronavirus disease-2019 (COVID-19): The epidemic and the challenges, Int. J. Antimicrob. Agents (2020) 105924.

[2] L.S. Wang, Y.R. Wang, D.W. Ye, Q.Q. Liu, A review of the 2019 Novel Coronavirus (COVID-19) based on current evidence, Int. J. Antimicrob. Agents 55 (6) (2020) 105948.

[3] WHO Director-General's opening remarks at the media briefing on COVID-19-11. https://www.who.int/dg/speeches/detail/who-director-general-s-opening-remarks-at-the-media-briefing-on-covid-19-11-march-2020.

[4] H. Nishiura, N.M. Linton, A.R. Akhmetzhanov, Early epidemiological assessment of the transmission potential and virulence of coronavirus disease 2019 (COVID-19) in Wuhan City, China, January–February, 2020, Int. J. Infect. Dis 93 (2020) 284–286.

[5] M. Hagar, H.A. Ahmed, G. Aljohani, O.A. Alhaddad, Investigation of some antiviral N-Heterocycles as COVID 19 drug: Molecular docking and DFT calculations, Int. J. Mol. Sci. 21 (2020) 3922.

[6] N. Zhu, D. Zhang, W. Wang, X. Li, B. Yang, J. Song, X. Zhao, B. Huang, W. Shi, R. Lu, et al., A Novel Coronavirus from patients with Pneumonia in China, 2019, N. Engl. J. Med 382 (2020) 727–733.

[7] P. Colson, J.M. Rolain, D. Raoult, Chloroquine for the 2019 novel coronavirus SARS-CoV-2, Int. J. Antimicrob. Agents 55 (3) (2020) 105923.

[8] P. Colson, J.M. Rolain, J.C. Lagier, P. Brouqui, D. Raoult, 2020. Chloroquine and hydroxychloroquine as available weapons to fight COVID-19, Int. J. Antimicrob. Agents 55 (4) (2020) 105932.

[9] M. Wang, R. Cao, L. Zhang, X. Yang, J. Liu, M. Xu, Z. Shi, Z. Hu, W. Zhong, G. Xiao, Remdesivir and chloroquine effectively inhibit the recently emerged novel coronavirus (2019-nCoV) in vitro, Cell Res. 30 (2020) 269–271.

[10] J. Pikkel, O. Chassid, A. Sharabi-Nov, I.B. Graef, A retrospective evaluation of the effect of hydroxyquinine on RPE thickness, Arch. Clin. Exp. Ophthalmol. 251 (2013) 1687–1690.

[11] C.R. Stelton, D.B. Connors, S.S. Walia, H.S. Walia, Hydrochloroquine retinopathy: characteristic presentation with review of screening, Clin. Rheumatol. 32 (2013) 895–898.

[12] J.J. Chen, R.M. Tarantola, C.N. Kay, V.B. Mahajan, Hydroxychloroquine (Plaquenil) Toxicity and Recommendations for Screening, Eye Rounds Org. (2011). http://EyeRounds.org/cases/139-plaquenil-toxicity.htm.

[13] E.B. Gouveia, M.S.A. Morales, G.B. Gouveia, V.P.M. Lourenzi, Ocular toxicity due to 4-aminoquinoline derivatives, Arq. Bras. Oftalmol. 70 (2007) 1046–1051.

[14] R.V. Shearer, E.L. Dubois, Ocular changes induced by long-term hydroxychloroquine therapy, Am. J. Ophthalmol. 64 (1967) 245–252.

[15] L.A. Percy, D. Pharm, M.A. Fang, The geropharmacology for the rheumatologist, Rheum. Dis. Clin. North Am. 46 (2000) 433–454.

[16] R. Goldhardt, Z.M.S. Corrêa, M.C. Eichenberg, I.M. Marcon, A. Vaccaro, Avaliação da toxicidade ocular por derivados da 4-aminoquinolona, Arq. Bras. Oftalmol. 65 (2002) 645–649.

[17] M.F. Marmor, U. Kellner, T.Y.Y. Lai, J.S. Lyons, W.F. Mieler, Revised recommendations on screening for chloroquine and hydroxychloroquine retinopathy, O. Amer. Acad. Ophthalmol. 118 (2011) 415–422.

[18] A.J. Flach, Improving the risk-benefit relationship and informed consent for patients treated with Hydroxychloroquine, Trans. Am. Ophthalmol. Soc. 105 (2007) 191–197.

[19] P. Gautret, J.-C. Lagier, P. Parolaa, V.T. Hoanga, L. Meddeba, M. Mailhea, B. Doudier, J. Courjone, V. Giordanengoh, V.E. Vieiraa, H. Tissot Dupont, S. Honoréi, P. Colsona, E. Chabrièrea, B. La Scolaa, J.-M. Rolaina, P. Brouqui, D. Raoult, Hydroxychloroquine and azithromycin as a treatment of COVID-19: results of an open-label nonrandomized clinical trial, Int. J. Antimicrob. Agents (2020).

[20] C. Biot, W. Daher, N. Chavain, T. Fandeur, J. Khalife, D. Dive, et al., Design and synthesis of hydroxyferroquine derivatives with antimalarial and antiviral activities, J. Med. Chem. 49 (2006) 2845–2849.

[21] M.F. Marmor, U. Kellner, T.Y. Lai, R.B. Melles, W.F. Mieler, American academy of ophthalmology. recommendations on screening for chloroquine and hydroxychloroquine retinopathy (2016 Revision), Ophthalmology 123 (6) (2016) 1386–1394.

[22] X. Yao, F. Ye, M. Zhang, C. Cui, B. Huang, P. Niu, et al., Vitro antiviral activity and projection of optimized dosing design of hydroxychloroquine for the treatment of severe acute respiratory syndrome coronavirus 2 (SARS-CoV-2), Clin. Infect. Dis. (2020) pii: ciaa237.

[23] S. Guiguere, S. Jacks, G. Roberts, Retrospective comparison azithromycin, claritromycin and erythromycin for treatmeant of foals with *Rodococcus equi* pneumonia, J. Vet. Intern. Med 18 (2004) 568–573.

[24] L.A. Hicks, T.H. Taylor, R.J. Hunkler, U.S. outpatient antibiotic prescribing, 2010, N. Engl. J. Med 368 (2013) 1461–1462.

[25] A.E. Girard, D. Girard, A.R. English, T.D. Gootz, C.R. Cimochowski, J.A. Faiella, et al., Pharmacokinetic and in vivo studies with azithromycin (CP-62,993), a new macrolide with an extended half-life and excellent tissue distribution, Antimicrob. Agents Chemother. 31 (1987) 1948–1954.

[26] G. Foulds, R.M. Shepard, R.B. Johnson, The pharmacokinetics of azithromycin in human serum and tissues, J. Antimicrob. Chemother. 25 (Suppl. A) (1990) 73–82.
[27] J.L. Blumer, Evolution of a new drug formulation: the rationale for high-dose, short-course therapy with azithromycin, Int. J. Antimicrob. Agents 3 (2005) S143–S147.
[28] R.I. Aminov, Biotic acts of antibiotics, Front. Microbiol. 4 (2013) 241.
[29] H.C. Steel, A.J. Theron, R. Cockeran, R. Anderson, C. Feldman, Pathogen- and host-directed anti-inflammatory activities of macrolide antibiotics, Mediat. Inflamm. (2012) 5842–5862.
[30] R. Danesi, A. Lupetti, C. Barbara, et al., Comparative distribution of azithromycin in lung tissue of patients given oral daily doses of 500 and 1000mg, J. Antimicrob. Chemother. 51 (4) (2003) 939–945.
[31] V. Rivulgo, M. Sparo, M. Ceci, E. Fumuso, A. Confalonieri, G. Delpech, S.F. Sanchez Bruni, Comparative plasma exposure and lung distribution of two human use commercial azithromycin formulations assessed in murine model: a preclinical study, BioMed. Res. Int. (2013), 392010.
[32] A.P. Kumar, J.H. Park, Azithromycin as a new chiral selector in capillary electrophoresis, J. Chromatogr. A 1218 (9) (2011) 1314–1317.
[33] A. Wildfeuer, H. Laufen, T. Zimmermann, Uptake of azithromycin by various cells and its intracellular activity under in vivo conditions, Antimicrob. Agents Chemother. 40 (1) (1996) 75–79.
[34] A.E. Girard, C.R. Cimochowski, J.A. Faiella, Correlation of increased azithromycin concentrations with phagocyte iniltration into sites of localized infection, J. Antimicrob. Chemother. 37 (1996) 9–19.
[35] K. Togami, S. Chono, K. Morimoto, Transport characteristics of clarithromycin, azithromycin and telithromycin, antibiotics applied for treatment of respiratory infections, in Calu-3 cell monolayers as model lung epithelial cells, Pharmazie 67 (5) (2012) 389–393.
[36] F. Imperi, L. Leoni, P. Visca, Antivirulence activity of azithromycin in Pseudomona aeruginosa Fontiers in Microbiology, Antimicrob. Resist. Chemother. 5 (1-6) (2014) 178.
[37] D.B. Kell, P.D. Dobson, S.G. Oliver, Pharmaceutical drug transport: the issues and the implications that it is essentially carrier-mediated only, Drug Discov. Today 16 (15-16) (2011) 704–714.
[38] H. Retallack, E. Di Lullo, C. Arias, K.A. Knopp, M.T. Laurie, C. Sandoval-Espinosa, et al., Zika virus cell tropism in the developing human brain and inhibition by azithromycin, Proc. Natl. Acad. Sci. U. S. A. 113 (50) (2016) 14408–14413.
[39] P.B. Madrid, R.G. Panchal, T.K. Warren, A.C. Shurtleff, A.N. Endsley, C.E. Green, A. Kolokoltsov, et al., Evaluation of ebola virus inhibitors for drug repurposing. ACS Infect. Dis 1 (7) (2015) 317–326.
[40] E. Bosseboeuf, M. Aubry, T. Nhan, J.J. de Pina, J.M. Rolain, D. Raoult, et al., Azithromycin inhibits the replication of Zika virus, J. Antivir. Antiretrovir 10 (1) (2018) 6–11.
[41] L.B. Bacharier, T.W. Guilbert, D.T. Mauger, S. Boehmer, A. Beigelman, A.M. Fitzpatrick, et al., Early administration of azithromycin and prevention of severe lower respiratory tract illnesses in preschool children with a history of such illnesses: a randomized clinical trial, JAMA 314 (19) (2015) 2034–2044.
[42] Y. Wan, J. Shang, R. Graham, R.S. Baric, F.J. Li, Receptor recognition by the novel coronavirus from Wuhan: an analysis based on decade-long structural studies of SARS coronavirus, Virology 94 (7) (2020).
[43] A.C. Walls, Y.-J. Park, M.A. Tortorici, A. Wall, A.T. McGuire, D. Veesler, Structure, function and antigenicity of the SARS-CoV-2 spike glycoprotein, BioRxiv (2020).
[44] D. Wrapp, N. Wang, K.S. Corbett, J.A. Goldsmith, C.-L. Hsieh, Olubukola Cryo-EM structure of the 2019-nCoV spike in the prefusion conformation, Science 367 (6483) (2020) 1260–1263.
[45] P. Zhou, X.-L. Yang, X.-G. Wang, B. Hu, L. Zhang, W. Zhang, H.-R. Si, Y. Zhu, B. Li, C.-L. Huang, et al., A pneumonia outbreak associated with a new coronavirus of probable bat origin, Nature 579 (2020) 270–273.
[46] M. Letko, A. Marzi, V. Munster, Functional assessment of cell entry and receptor usage for SARS-CoV-2 and other lineage B betacoronaviruses, Nat. Microbiol. 5 (2020) 562–569.
[47] P. Eleftheriou, D. Amanatidou, A. Petrou, A. Geronikaki, Silico evaluation of the effectivity of approved protease inhibitors against the main protease of the novel SARS-CoV-2 virus, Molecules 25 (2020) 2529.
[48] L. Zhang, D. Lin, X. Sun, U. Curth, C. Drosten, L. Sauerhering, S. Becker, K. Rox, R. Hilgenfeld, Crystal structure of SARS-CoV-2 main protease provides a basis for design of improved a-ketoamide inhibitors, Science 368 (6489) (2020) 409–412.
[49] M. Drag, G.S. Salvesen, Emerging principles in protease-based drug discovery, Nat. Rev. Drug Discov. 9 (2010) 690–701.
[50] Y. Wang, Q. Liu, L. Qui, T. Wang, T. Yuan, J. Lin, S. Luo, Molecular structure, IR spectra, and chemical reactivity of cisplatin and transplatin: DFT studies, basis set effect and solvent effect, Spectrochim. Acta A 150 (2015) 902–908.
[51] M.M. Bilkan, Experimental, Theoretical studies on theobromine and theobromine-water complexes, AKU J. Sci. Eng. 18 (2018), 011106 (90-102).
[52] R. Carrasco-velar, J.A. Padron, J. Galvez, Definition of a novel atomic index for QSAR: the refractotopological state, J. Pharmaceut. Sci. 7 (2004) 19–26.
[53] V.R. Murthy, D.V. Raghuram, P.N. Murthy, Drug, dosage, activity, studies antimalarials by physical methods–II. Biomed, Inform. Publ. Group 2 (1) (2007) 12–16.
[54] M.F. Costa, A theoretical study of 1,4-bis (3-carboxy-3-oxo-prop-1-enyl) benzene I. Ciencias Exatas e Tecnologicas,, Londrina 31 (1) (2010) 31–36.
[55] M.J. Frisch, G.W. Trucks, H.B. Schlegel, G.E. Scuseria, M.A. Robb, J.R. Cheeseman, G. . Scalmani, V. Barone, B. Mennucci, G.A. Petersson, H. Nakatsuji, M. Caricato, X. Li, H.P. Hratchian, A.F. Izmaylov, J. Bloino, G. Zheng, J.L. Sonnenberg, M. Hada, M. Ehara, K. Toyota, R. Fukuda, J. Hasegawa, M. Ishida, T. Nakajima, Y. Honda, O. Kitao, H. Nakai, T. Vreven, J.A. Montgomery Jr., J.E. Peralta, F. Ogliaro, M. Bearpark, J.J. Heyd, E. Brothers, K.N. Kudin, V.N. Staroverov, T. Keith, R. Kobayashi, J. Normand, K. Raghavachari, A. Rendell, J.C. Burant, S.S. Iyengar, J. Tomasi, M. Cossi, N. Rega, J.M. Millam, M. Klene, J.E. Knox, J.B. Cross, V. Bakken, C. Adamo, J. Jaramillo, R. Gomperts, R.E. Stratmann, O. Yazyev, A.J. Austin, R. Cammi, C. Pomelli, J.W. Ochterski, R.L. Martin, K. Morokuma, V.G. Zakrzewski, G.A. Voth, P. Salvador, J.J. Dannenberg, S. Dapprich, A.D. Daniels, O. Farkas, J.B. Foresman, J.V. Ortiz, J. Cioslowski, D.J. Fox, Gaussian 09, Revision D.01, Gaussian, Inc., Wallingford CT, 2010.
[56] D.R. Dennington, T. Keith, J. Miller, GaussView, Version 5.0.8, Semichem Inc., Shawnee Mission KS, 2008.
[57] A.A. Alex, Quantum mechanical calculations in medicinal chemistry: relevant method or a quantum leap too far? in: John B. Taylor, David J. Triggle (Eds.), Comprehensive Medicinal Chemistry Elsevier, Oxford (, 2007, p. 379.
[58] A.H. Reshak, N.M. Abbass, J. Bíla, M.R. Johan, I. Kityk, Noncentrosymmetric Sulfade Oxide MZnSO (M = Ca or Sr) with strongly polar structure as novel nonlinear crystals, J. Phys. Chem. C 123 (44) (2019) 27172–27180. ISSN 1932–7447.
[59] A.H. Reshak, S. Auluck, The influence of oxygen vacancies on the linear and nonlinear optical properties of Pb7O(OH)3(CO3)3(BO3), RSC Adv 7 (2017) 14752–14760.
[60] G.W. Ejuh, F. Tchangnwa Nya, N. Djongyang, J.M.B. Ndjaka, Study of some properties of quinone derivatives from quantum chemical calculations, Opt. Quant. Electron 50 (9) (2018) 336 (1-19).
[61] G.W. Ejuh, S. Nouemo, F. Tchangnwa Nya, J.M.B. Ndjaka, Computational determination of the electronic and nonlinear optical properties of the molecules 2-(4-aminophenyl) Quinoline, 4-(4-aminophenyl) quinoline, anthracene, anthraquinone and phenanthrene, Mater. Lett. 178 (2016) 221–226.
[62] G.W. Ejuh, J.M.B. Ndjaka, A.N. Singh, Study of the structures and Physico-chemical properties of the molecules Pyrimethamine and Sulfadoxine by ab initio and DFT methods, Canadian J. Pure Appl. Sci. 5 (2) (2011), 1591-1532.
[63] A. Semeniuk, J. Justyna Kalinowska-Tluscik, W. Nitek, B.J. Oleksyn, Intermolecular interactions in crystalline hydroxychloroquine sulfate in comparison with those in selected antimalarial drugs, J. Chem. Crystallogr 38 (5) (2008) 333–338.
[64] E. Eroglu, H. Türkmen, A DFT-based quantum theoretic QSAR study of aromatic and heterocyclic sulfonamides as carbonic anhydrase inhibitors against isozyme, Ca-Ii, J. Mol. Graph. Model 26 (2007) 701.
[65] S.M. LaPointe, D.F. Weaver, A review of density functional theory quantum mechanics as applied to pharmaceutically relevant systems, Curr. Comput. Aided Drug Des. 3 (2007) 290.
[66] A.M. Ferreira, M. Krishnamurthy, B.M. Moore Ii, D. Finkelstein, D. Bashford, Quantitative structure–activity relationship (QSAR) for a series of novel cannabinoid derivatives using descriptors derived from semi-empirical quantum-chemical calculations, Bioorg. Med. Chem. 17 (2009) 2598.
[67] S. Agatonovic-Kustrin, R. Beresford, A.P.M. Yusof, Theoretically-derived molecular descriptors important in human intestinal absorption, J. Pharmaceut. Biomed. Anal. 25 (2001) 227.
[68] A.M. Matuszek, Defining Known Drug Space By DFT Based Molecular Descriptors. Virtual Screening for Novel Atg5-Atg16 Complex Inhibitors for Autophagy Modulation, Ph.D Thesis, 2014, http://researchspace.auckland.ac.nz/feedback.
[69] D. Kanis, M. Ratner, T. Marks, Polarizaability and hyperpolarizability calculation, Chem. Rev. 94 (1994) 239.
[70] C. Gu, X. Jiang, X. Ju, G. Yu, Y. Bian, Qsars for the toxicity of polychlorinated dibenzofurans through Dft-calculated descriptors of polarizabilities, hyperpolarizabilities and hyper-order electric moments, Chemosphere 67 (2007) 1325.
[71] N.M. O'Boyle, A.L. Tenderholt, K.M. Langner, A library for package-independent computational chemistry algorithms, J. Comput. Chem. 29 (2008) 839–845.
[72] H. Tanak, Quantum chemical computational studies on 2-methyl-6-[2-(trifluoromethyl) phenyliminomethyl]phenol, J. Mol. Struct. Theochem. 950 (1) (2010) 5–12.
[73] J. Turner, D. Maddalena, S. Agatonovic-Kustrin, Bioavailability prediction based on molecular structure for a diverse series of drugs, Pharmaceut. Res. 21 (2004) 68.
[74] M. Hutter, Prediction of blood–brain barrier permeation using quantum chemically derived information, J. Comput. Aided Mol. Des 17 (2003) 415.
[75] Y. Tadjouteu Assatse, G.W. Ejuh, R.A. Yossa Kamsi, F. Tchoffoa, J.M.B. Ndjaka, Theoretical studies of nanostructures modeled by the binding of Uracil derivatives to functionalized (5,5) carbon nanotubes, Chem. Phys. Lett. 731 (2019) 136602.
[76] J.B. Fankam Fankam, G.W. Ejuh, F. Tchangwa Nya, J.M.B. Ndjaka, Theoretical investigation of the molecular structure, vibrational spectra, thermodynamic and nonlinear optical properties of 4, 5dibromo2, 7dinitro fluorescein, Opt. Quant. Electron. 52 (2020) 292.
[77] C. Fonkem, G.W. Ejuh, F. Tchangnwa Nya, R.A. Yossa Kamsi, J.M.B. Ndjaka, Theoretical study of optoelectronic properties of the molecule 2-cyano-3- [4-(diphenylamino) phenyl] acrylic acid, J. Iran. Chem. Soc. 17 (3) (2019) 533–543.
[78] A. Veved, G.W. Ejuh, N. Djongyang, Effect of HfO2 on the dielectric, optoelectronic and energy harvesting properties of PVDF, Opt. Quant. Electron. 23 (10) (2019).

[79] R.A. Yossa Kamsi, G.W. Ejuh, Y. Tadjouteu Assatse, C.N. Njeumen, F. Tchoffo, J.M.B. Ndjaka, Computational study of reactivity and solubility Rubescin D and E in gas phase and in solvent media using Hatre - Fock and DFT method, Chin. J. Phys. 60 (2019) 1–11.

[80] G.I. Livshits, A. Stern, D. Rotem, N. Borovok, G. Eidelshtein, A. Migliore, E. Penzo, S.J. Wind, R. Di Felice, S.S. Skourtis, J.C. Cuevas, L. Gurevich, A.B. Kotlyar, D. Porath, Long-range charge transport in single G-quadruplex DNA molecules, Nat. Nanotechnol. 9 (2014) 1040–1046.

[81] N.C. Garbett, J.B. Chaires, Thermodynamic studies for drug design and screening, Expert Opin. Drug Discov. 7 (4) (2012) 299–314.

[82] G.A. Holdgate, Thermodynamics of binding interactions in the rational drug design process, Expert Opin. Drug Discov. 2 (8) (2007) 1103–1114.

[83] G.A. Holdgate, W.H.J. Ward, Measurements of binding thermodynamics in drug discovery, Drug Discov. Today 10 (22) (2005) 1543–1550.